First-Principles Study of the Optical Dipole Trap for Two-Dimensional Excitons in Graphane

Hiroki Katow,[1] Ryosuke Akashi,[2] Yoshiyuki Miyamoto,[3] and Shinji Tsuneyuki[2]
[1]*Photon Science Center, Graduate School of Engineering, The University of Tokyo, Bunkyo-ku, Tokyo 113-8656, Japan*
[2]*Department of Physics, The University of Tokyo, 7-3-1 Hongo, Bunkyo-ku, Tokyo 113-0033, Japan*
[3]*Research Center for Computational Design of Advanced Functional Materials, National Institute of Advanced Industrial Science and Technology (AIST), Central 2, Tsukuba, Ibaraki 305-8568, Japan*

(Received 12 November 2020; revised 31 March 2022; accepted 13 June 2022; published 18 July 2022)

Recent studies on excitons in two-dimensional materials have been widely conducted for their potential usages for novel electronic and optical devices. Especially, sophisticated manipulation techniques of quantum degrees of freedom of excitons are in demand. In this Letter we propose a technique of forming an optical dipole trap for excitons in graphane, a two-dimensional wide gap semiconductor, based on first-principles calculations. We develop a first-principles method to evaluate the transition dipole matrix between excitonic states and combine it with the density functional theory and GW + BSE calculations. We reveal that in graphane the huge exciton binding energy and the large dipole moments of Wannier-like excitons enable us to induce the dipole trap of the order of meV depth and μm width. This Letter opens a new way to control light-exciton interacting systems based on newly developed numerically robust *ab initio* calculations.

DOI: 10.1103/PhysRevLett.129.047401

The exciton is a quasiparticle formed by a pair consisting of an electron and a hole. The binding and relaxation processes of the exciton dominate the optical response of the semiconductors. Optical control of excitons via the strong light-exciton coupling is particularly an intriguing subject for its application to optical devices. For example, through the studies on transition metal dichalcogenides (TMDs), the valley-selective formation of the excitons by circularly polarized light and their transport have been intensively pursued [1,2]. Further sophistication of the exciton manipulating techniques will benefit the future development of the field.

The subject of this Letter is a spatial control of the center-of-mass (c.m.) motion of the excitons. Let us list a few pioneering studies on this: applying a uniaxial strain potential by mechanical force [3,4], stacking periodic metallic gates on a quantum well [5], utilizing a repulsive potential between spatially indirect excitons [6–8], inducing a periodic strain field by surface acoustic waves (SAWs) [9–11], utilizing the Pauli repulsion between virtually excited excitons [12–14], and making use of the optical Stark shift of trion resonance for trapping of free carriers [15]. The moiré pattern, which is formed by piling up two TMD monolayers with incommensurate angle, is predicted to confine excitons [16–19] and the experimental signatures have been observed [20–23].

Here, we consider application of the idea in the research field of ultracold atomic systems. A rich variety of electromagnetic techniques have been implemented for designing the geometry of the confinement potential, which have been already applied to the studies on quantum many-body phases like the atomic BEC and the quantum simulator [24,25]. A representative confinement mechanism in practice is the energy level shift induced by electromagnetic fields; this is called optical dipole trap. Our central object is to propose the optical dipole trapping phenomenon in the excitonic system, which could provide us with precise nonmechanical control of the excitons like that of the cold atomic systems.

In this Letter we theoretically propose an optical control of exciton c.m. motion in graphane (hydrogen-terminated graphene), a two-dimensional wide gap semiconductor. The optical potential for the excitons in graphane can be implemented as a spatial energy shift of the exciton dressed state which is formed by irradiating external laser fields. We show that two- and three-level systems are well defined in this system with the use of first-principles methods, namely, the density functional theory (DFT), GW approximation, and the Bethe-Salpeter equation. The dressed states are parametrized by the electronic transition dipole moment and energy level configuration of graphane excitons. The dipole parameter in the Bloch representation requires derivatives in the reciprocal space, which generally suffers from the gauge dependence. We constructed a gauge-free formula for the transition matrix element between the excitonic states via the optical dipole interaction, which is an intuitive extension of the King-Smith–Vanderbilt (KS–V) formula for electronic polarizability calculations in ground states [26,27]. We found that some features of graphane excitons—huge binding energy, wide energy

level spacing, and large transition dipole moment—yield the deep potential shift of order of meV without violating the rotational wave approximation [24,25]. These features are common in two-dimensional semiconductors such as TMDs. Thus we can expect a wide application of this technique.

We begin with a general introduction of laser-matter interaction in a few-level system with the dipole approximation. In particular we consider a specific three-state system where two out of three levels are degenerate, which is later seen to correspond to graphane. Applying the rotational wave approximation, the system is described by the Rabi Hamiltonian H_R. Eigenstates of H_R are called dressed states. The Rabi Hamiltonian of a two-level system $H_R^{(2)}$ and its eigenvalues $E^{\pm}$ are given by

$$H_R^{(2)} = \begin{pmatrix} -\Delta & -\Omega_R/2 \\ -\Omega_R^*/2 & 0 \end{pmatrix} \tag{1}$$

$$E_{\pm} = -1/2\{\Delta \pm (\Delta^2 + |\Omega_R|^2)^{1/2}\}, \tag{2}$$

in atomic unit. Here Δ is detuning and $\Omega_R = 2\boldsymbol{E}\cdot\boldsymbol{d}_{12}$ is the Rabi frequency. $\boldsymbol{E}$ is a local external field and $\boldsymbol{d}_{12}$ is electric transition dipole moment which is defined by a matrix $\boldsymbol{d}_{S'S} = \langle S'|\boldsymbol{r}|S\rangle$ where $|S(S')\rangle$ is the excitonic eigenstate. In the same way, the Rabi Hamiltonian of a three-level system $H_R^{(3)}$ and corresponding eigenvalues are derived as follows:

$$H_R^{(3)} = \begin{pmatrix} 0 & 0 & \Omega_{13}/2 \\ 0 & 0 & \Omega_{23}/2 \\ \Omega_{13}^*/2 & \Omega_{23}^*/2 & -\Delta \end{pmatrix} \tag{3}$$

$$E_{0,\pm} = 0, -1/2\{\Delta \pm (\Delta^2 + |\Omega_{13}|^2 + |\Omega_{23}|^2)^{1/2}\}. \tag{4}$$

Here $\Omega_{13(23)} = 2\boldsymbol{E}\cdot\boldsymbol{d}_{13(23)}$ is the Rabi frequency. We assumed that among three excitonic states $|S\rangle$ ($S = 1, 2, 3$) the first two are degenerate. Thus in both cases the system is parametrized by $\boldsymbol{E}$, Δ, and $\boldsymbol{d}$. The transition dipole moment $\boldsymbol{d}$, being the only intrinsic quantity, must be given by *ab initio* calculations. We referred to [24,25] for above formulations. $U_{\mathrm{op}}^{\pm} = E_{\pm}(\boldsymbol{E}) - E_{\pm}(\boldsymbol{0})$ gives optical potential depth which moderately varies in the spatial scale of laser wave length as $U_{\mathrm{op}}^{\pm}(\boldsymbol{r})$.

Calculation of the dipole moment in a periodic system needs special care as there is an ambiguity in the definition of the unit cell boundary and the dependence on a gauge of the Kohn-Sham orbital. King-smith and Vanderbilt have reformulated the Berry phase formula for the electric polarization of dielectrics which is free from the choice of gauge [26,27]. A similar problem is present in the transition dipole moment of the excitonic eigenstates in the periodic system. In this Letter we extend the KS–V formula for excitonic systems as follows:

$$d\boldsymbol{k}\cdot\langle S'|\boldsymbol{r}|S\rangle \simeq \sum_{\boldsymbol{k}_\perp} \Im\left[\ln\prod_{\boldsymbol{k}_\parallel}\det\{T_{e^-}^{SS'} + W_{e^-}\} - \ln\prod_{\boldsymbol{k}_\parallel}\det\{T_{h^+}^{SS'} + W_{h^+}\}\right]. \tag{5}$$

Here $|S\rangle = \sum A_{kvc}^{s} a_{kc}^{\dagger} a_{kv}|\mathrm{gs}\rangle$ is an excitonic state and $|\mathrm{gs}\rangle$ indicates the ground state,

$$T_{e^-,c_1c_2}^{S'S} = \sum_{c_3}^{N_c}\sum_{v}^{N_v} A_{\boldsymbol{k},vc_3}^{S'*} A_{\boldsymbol{k},vc_1}^{S} \langle u_{\boldsymbol{k},c_3}|u_{\boldsymbol{k}+d\boldsymbol{k},c_2}\rangle \tag{6}$$

$$T_{h^+,v_1v_2}^{S'S} = \sum_{c}^{N_c}\sum_{v_3}^{N_v} A_{\boldsymbol{k},v_1c}^{S'*} A_{\boldsymbol{k},v_3c}^{S} \langle u_{\boldsymbol{k},v_3}|u_{\boldsymbol{k}+d\boldsymbol{k},v_2}\rangle \tag{7}$$

$$W_{e^-(h^+)mn} = \delta_{mn}\langle u_{\boldsymbol{k},m}|u_{\boldsymbol{k}+d\boldsymbol{k},m}\rangle/|\langle u_{\boldsymbol{k},m}|u_{\boldsymbol{k}+d\boldsymbol{k},m}\rangle|. \tag{8}$$

$|u_{\boldsymbol{k},m}\rangle$ is a cell periodic factor of the Kohn-Sham orbital. N_c is the number of conduction bands and N_v is the number of valence bands. The product $\prod_{\boldsymbol{k}_\parallel}$ is taken along a closed path parallel to $d\boldsymbol{k}$ in the BZ and $\sum_{\boldsymbol{k}_\perp}$ sums up all the paths. $d\boldsymbol{k}$ is a vector whose norm is equal to the k point spacing and is parallel to reciprocal lattice vectors in our calculation. The index of the matrices with a subscript e^- (h^+) runs over conduction (valence) bands. Equation (5) still possesses a multivalued nature of the logarithm given by an integer multiple of 2π. Its contribution can be omitted as long as we sample a large number of k points. See Ref. [28] for details, which also refers to a related work [29].

Graphane is a two-dimensional wide gap semiconductor composed of hydrogenated graphene. Amongst possible metastable states, the *chair-type* conformation is reported to be most stable [30]. Some groups have reported the hydrogenation of free-standing graphene [31,32]. We show the crystal and DFT band structure of *chair-type* graphane in Figs. 1(a) and 1(b). Graphane possesses D_{3d} group symmetry and hence has no permanent dipole. Accordingly the degree of the degeneracy cannot be more than double,

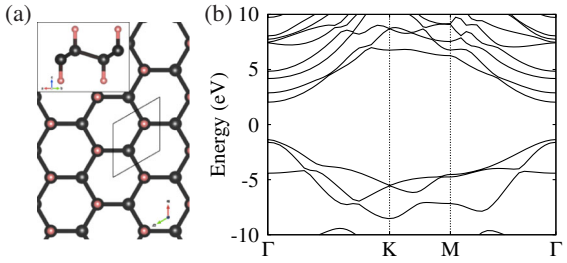

FIG. 1. (a) The crystal structure of the chair-type graphane seen from (001) direction and (110) direction (inset). The black (pink) balls indicate carbon (hydrogen) atoms. A wedge-shaped area indicates a unit cell. (b) The band structure of the graphane calculated by using the local density approximation.

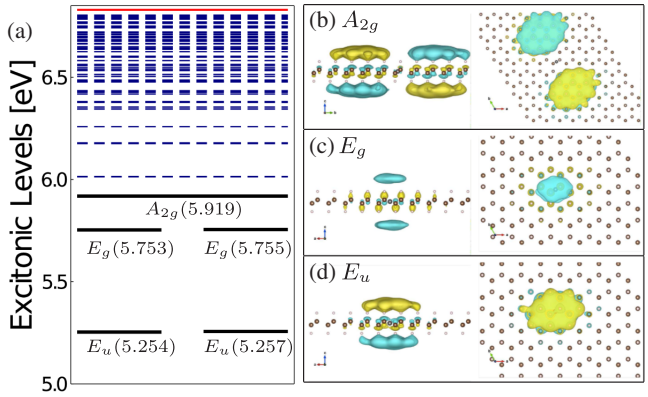

FIG. 2. (a) Excitonic levels measured from the valence band maximum (VBM) in eV on the Γ point. Characters of the D_{3d} group, which each level belongs to, are shown for the first five levels with its energy in brackets. The CBM is at 6.8 eV and shown by a red solid line. The real part of the excitonic wave function is depicted for (b) the A_{2g} exciton, (c) E_g exciton, and (d) the E_u exciton from (100) (left panel) and (001) (right panel) directions. Hole coordinates are fixed in the middle of C—C bonding. Two colors of isosurface indicate the sign of wave functions.

which greatly simplifies further analysis. A direct Kohn-Sham gap opens at Γ point whose width is 3.4 eV. DFT calculation was done by Quantum-ESPRESSO package [33] with $18 \times 18 \times 1$ k points and 150 Ry energy cutoff. A PBE-type energy density functional was used [34,35]. The interlayer spacing is 15 Å. It is well known that the DFT calculation systematically underestimates the energy gap. We therefore implemented energy level calculations based on GW approximation which takes the screening effect by medium into account. The GW calculation and subsequent BSE calculation were done by using BerkeleyGW code [36]. The resulting energy band gap is 6.8 eV. Detailed calculation conditions and the band gap convergence is summarized in the Supplemental Material [28] in comparison with preceding works [37–40].

A typical feature of two-dimensional semiconductors is the weak screening of Coulomb interaction by medium which leads to the formation of excitons with huge binding energy. In Fig. 2(a) energy levels calculated by the GW + BSE method with the Tamm-Dancoff approximation [41] are plotted. We used a $36 \times 36 \times 1$ k point mesh. The lowest five levels are highlighted by bold black lines as we focus on the manipulation of low energy levels. These five levels belong to characters E_u, E_g, and A_{2g} of the D_{3d} group. E_u and E_g states are plotted by short lines to emphasize the double degeneracy. The E_u exciton possesses huge binding energy which amounts to 1.6 eV measured from the conduction band minimum (CBM) given by the GW calculation. In Figs. 2(b)–2(d), the real part of the excitonic wave functions for the lowest five levels is shown. The E_u exciton in this Letter obviously corresponds to A and B excitons in [37]. See also Ref. [42].

TABLE I. The traces of $D_{ij} = d^{i\dagger}d^j$, $(i, j = x, y, z)$, where D_{ij} is a 2×2 or 2×1 matrix in our case. $\mathrm{tr}D_{ij}$ is invariant under a unitary transformation of excitonic states.

S	S'	$\sqrt{\mathrm{tr}D_{xx}}$	$\sqrt{\mathrm{tr}D_{yy}}$	$\sqrt{\mathrm{tr}D_{zz}}$
E_u	E_g	0.17	0.12	4.59
E_u	A_{2g}	6.75	6.54	0.00

The resulting transition dipole moments $\boldsymbol{d}_{SS'}$ for $S = E_u$ and $S' = E_g, A_{2g}$ are summarized in Table I. When the system possesses time-inversion symmetry, the dipole matrix can always be taken as real. The determinant and trace of a matrix $D_{ij} = d^{i\dagger}d^j$ $(i, j = x, y, z)$ are unitarily invariant. The D_{3d} group symmetry requires $\mathrm{tr}D_{xx} = \mathrm{tr}D_{yy}$; we specified the detailed calculation condition so that this relation is optimally satisfied [28]. The values are comparable with those of the excitonic system in quantum dots and one order larger than atomic systems [43,44]. As for the dipole matrix of the E_u and E_g states, the z component is dominant and in-plane component is negligible. The dipole matrix is block diagonal and split into two 2×2 matrices. This block diagonalization can always be done by a unitary transformation, and thus we can construct two two-level systems from the E_u and E_g excitons. The E_u and A_{2g} excitons form a three-level system and in-plane dipole matrices dominate in contrast to the previous case. The second E_g state is present 100 meV above the A_{2g} state and it provides an upper limit of the applicable field strength within the rotational wave approximation. In later discussions, we consider two- and three-level systems using the $E_u - E_g$ and $E_u - A_{2g}$ excitonic levels, respectively.

Now we show the polarization dependency of the potential depth U^+_{op} on a unit sphere in Fig. 3 for the red detuning $\Delta = -10$ meV. With this detuning value, U^+_{op} becomes an attractive potential whose maximum depth reaches a few meV. This is comparable with the strain-induced potential in bulk crystal [3,4]. Even in this condition, the Rabi frequency Ω_R and detuning Δ are far smaller than the energy level spacing ω, which validates the rotational wave approximation. It is by virtue of the following two factors: (i) large transition dipole moment and (ii) huge energy level spacing. Particularly the factor (ii) owes to the weak screening of Coulomb potential unique in low-dimensional systems. Another illuminating feature is the anisotropy of U^+_{op} as a consequence of the anisotropic dipole. In Fig. 3(a) U^+_{op} reaches maximum depth when the polarization vector of light is oriented normal to the crystal plane. In this level configuration the external field does not break pseudospin symmetry of the E_u exciton. In the $E_u - A_{2g}$ three level system, the transition dipole is oriented along the crystal plane. Significantly, the degeneracy is broken in this system; it could open up a way to manipulate the pseudospin degrees of freedom of the E_u exciton like the stimulated Raman

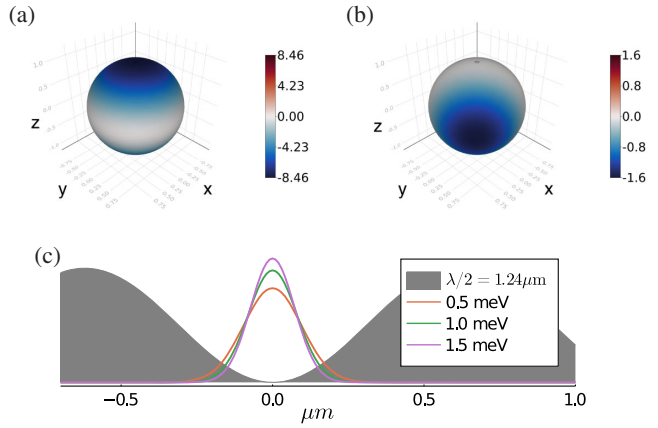

FIG. 3. Polarization angle dependency of the U^{+}_{opt} for (a) two-level system and (b) three-level system in units of meV plotted on a unit sphere by using Makie.jl [46]. The former is composed of the E_u and E_g excitons, and the latter is composed of the E_u and A_{2g} excitons. The field intensity is 3.51×10^8 W/cm^2 in (a), and 1.00×10^7 W/cm^2 in (b). The detuning $\Delta = -10$ meV in both (a) and (b). The z axis is taken to be normal to the crystal plane. (c) Square of the c.m. wave function $|\psi_{\mathrm{c.m.}}(\boldsymbol{r}_{\mathrm{c.m.}})|^2 \propto \exp\{-r^2_{\mathrm{c.m.}}/R^2\}$ for three U^{+}_{opt} values in the $E_u - E_g$ two-level system. $R = 0.135$, 0.113, 0.102 μm for $U^{+}_{\mathrm{opt}} = 0.5$, 1.0, 1.5 meV, respectively. The blue line is the spatial profile of $U^{+}_{\mathrm{op}}(\boldsymbol{r})$ with wave length $\lambda = 1.24$ μm just for a guide to the eye.

adiabatic passage (STIRAP) [24,25,45] besides possible pseudospin selective trapping. We note that the angular dependency is unitary invariant in Fig. 3 while the bases to span the dressed states depend on the mixing of degenerate E_u states in each BSE calculation.

Here we consider some obstacles to the optical dipole trap. A major process that could disrupt the trapping is the radiation heating by the recoil energy E_{rec} of the single photon emission process. Cudazzo *et al.* [47] theoretically found that the dispersion relation of the graphane exciton is well approximated by a quadratic curve with effective exciton mass $m_{\mathrm{exc}} \sim 1.8 m_{e^-}$ where m_{e^-} is the free electron mass. E_{rec} can then be of the order of $\hbar^2 \boldsymbol{K}^2/2m_{\mathrm{exc}} = 1.36 \times 10^{-4}$ meV for the $E_g \to E_u$ de-excitation where $\boldsymbol{K}$ is the momentum of a photon. The net influx of recoil energy R_{heat} in unit time to the E_u exciton can be approximated by a product of the inverse lifetime Γ of de-excitation and the occupation ρ of E_g exciton in a dressed state as $R_{\mathrm{heat}} \sim E_{\mathrm{rec}} \rho \Gamma$. On the basis of the first-principles calculation [37] and summing up the contributions from the de-excitation processes from the E_g to E_u exciton states with respect to the momentum transfer $\boldsymbol{q}$, we obtain $\Gamma = 5e^2 d^2 \omega^3/3\hbar c^3$ and consequently its lifetime $\tau = 3.5 \times 10^2$ ns. This is much longer than the lifetime of the E_u exciton, estimated to be 15 ps [37]; we thus conclude that the radiation heating effect is irrelevant since it is negligibly small in the time scale of the exciton lifetime.

Another concern is the distance an exciton can travel. When you apply a standing wave of monochromic laser, it serves as a potential whose periodicity is half a wave length, which in this case would be around 1 μm. This scale is comparable with the typical size of monolayer crystal flakes of two-dimensional materials available experimentally [48–54]. The spatial extension of the c.m. motion of the trapped exciton depends on the optical potential depth. As a rough estimation we approximate the optical dipole trap by a 1D harmonic potential as $U^{+}_{\mathrm{opt}} \cos(2\pi r/\lambda) \simeq U^{+}_{\mathrm{opt}}\{1 - (2\pi r/\lambda)^2/2\}$ with the radial coordinate r, where $\lambda \sim 1.24$ μm for the $E_u - E_g$ system. Then the radius R of the c.m. wave function $\psi_{\mathrm{cm}}(\boldsymbol{r}_{\mathrm{cm}})$ ($|\psi_{\mathrm{c.m.}}(\boldsymbol{r}_{\mathrm{c.m.}})|^2 \propto \exp\{-r^2_{\mathrm{c.m.}}/R^2\}$) becomes $R = 0.137$ μm for $|U^{+}_{\mathrm{op}}| = 0.5$ meV [Fig. 3(c)]. According to the experimental studies on low dimensional systems [55–59], the exciton diffusion coefficient ranges from $O(10^{-1})$ to $O(10^2)$ cm^2/s. Within the expected graphane exciton lifetime $\tau = 15$ ps [37], excitons would then be transported by sub-μm. This is comparable enough with the radius R. It will lead to the formation of a bright spot due to the de-excitation-induced light emission.

We also consider obstacles in solids. We discuss interactions with the edge states, defects, impurities, and substrates. According to the first-principles studies [60–62], those states spatially extend over few unit cells and are electronically neutral. Excitons trapped in interior regions far from the crystal boundary will not be seriously affected by the edge state. In contrast, the defects and impurities may deeply capture excitons, which, in turn, would be easily distinguished from optically trapped excitons because of the largely shifted energy levels and small density of states. As the Pauli blocking effect hinders the capturing process, we expect the free exciton density should be roughly one order larger than the defect and impurity density. We also note the many-body screening would provide an upper limit of the free exciton density. Katsch *et al.* [63] estimated that the exciton energy level shift reaches 2.0 meV when the exciton density is sub-10^{12} cm^{-2} in TMDs. Since the graphane exciton is more tightly bound, the shift will be smaller for the same excitation density. Unless the exciton density becomes larger than 10^{11} cm^{-2}, the many-body screening would not dominate over the optical trapping. The screening effect by substrate in two-dimensional materials causes significant band gap renormalization [64,65]. Supposedly the graphane mounted on a substrate shows strong renormalization. As long as the renormalization uniformly scales the whole exciton energy spectrum, our trapping mechanism will not be essentially modified, while the maximum potential depth will be reduced by the same scaling factor. We lastly note that the exciton-phonon interaction [66] possibly works as either a heating or cooling process. Because *ab initio* calculations of the exciton-phonon scattering ratio

in monolayers are numerically too demanding, its analysis is left for future studies.

In conclusion, we theoretically investigated the feasibility of a novel optical technique to manipulate the c.m. and pseudospin degrees of freedom of excitons in graphane. We first employed the GW + BSE calculation in combination with DFT to determine model parameters. We found that the E_u, E_g, and A_{2g} excitons form suitable level configurations since they are well isolated from adjacent levels. We also developed a theoretical method to compute the electronic transition dipole moment between excitonic states which is analogous to the Berry phase formula for ground states of periodic systems. Our formulation is free from the choice of gauge of Kohn-Sham orbitals and hence essential to obtain the dipole matrix of exciton in periodic systems. The dipole moments of the graphane exciton are one order larger than those of atomic systems and surely merit the implementation of optical potential. The two dimensionality of the graphane leads to anisotropic dipoles. In consequence, the application of a normal-to-plane polarized field equally traps the degenerate pair of E_u excitons, while the in-plane polarized field breaks this degeneracy, which works as a pseudospin-selective potential. The potential shape can be arbitrarily designed by the spatial profile of the laser field. We expect that such a technique advances the research of pseudospin dynamics and many-body physics of excitons.

We expect the trapping mechanism also works for other compounds. TMDs and h-BN show a nonparabolic exciton dispersion, strong spin-orbit coupling, and strong dependence of the exciton inner structure on c.m. motion [47,67]. A more complete description of those effects is our future work. Our gauge-free formulation of the exciton transition dipole moment provides a basic platform for exploring optical exciton manipulation technologies. Dark exciton trapping with the aid of permitted inter-dark-state transitions deserves a special mention, which is likely promising due to its long lifetime [68,69].

Part of this work is based on the results obtained from the NEDO project "Development of advanced laser processing with intelligence based on high-brightness and high-efficiency laser technologies" (TACMI project).

[1] J. R. Schaibley, H. Yu, G. Clark, P. Rivera, J. S. Ross, K. L. Seyler, W. Yao, and X. Xu, Nat. Rev. Mater. **1**, 16055 (2016).
[2] G. Wang, A. Chernikov, T. F. Heinz, X. Marie, T. Amand, and B. Urbaszek, Rev. Mod. Phys. **90**, 021001 (2018).
[3] R. Balili, V. Hartwell, D. Snoke, L. Pfeiffer, and K. West, Science **316**, 1007 (2007).
[4] K. Yoshioka, E. Chae, and M. Kuwata-Gonokami, Nat. Commun. **2**, 328 (2011).
[5] C. W. Lai, N. Y. Kim, S. Utsunomiya, G. Roumpos, H. Deng, M. D. Fraser, T. Byrnes, P. Recher, N. Kumada, T. Fujisawa, and Y. Yamamoto, Nature (London) **450**, 529 (2007).
[6] A. Amo, S. Pigeon, C. Adrados, R. Houdrè, E. Giacobino, C. Ciuti, and A. Bramati, Phys. Rev. B **82**, 081301(R) (2010).
[7] E. Wertz, L. Ferrier, D. D. Solnyshkov, R. Johne, D. Sanvitto, A. Lematre, I. Sagnes, R. Grousson, A. V. Kavokin, P. Senellart, G. Malpuech, and J. Bloch, Nat. Phys. **6**, 860 (2010).
[8] A. T. Hammack, M. Griswold, L. V. Butov, L. E. Smallwood, A. L. Ivanov, and A. C. Gossard, Phys. Rev. Lett. **96**, 227402 (2006).
[9] M. J. A. Schuetz, J. Knörzer, G. Giedke, L. M. K. Vandersypen, M. D. Lukin, and J. I. Cirac, Phys. Rev. X **7**, 041019 (2017).
[10] M. M. de Lima, M. vander Poel Jr., P. V. Santos, and J. M. Hvam, Phys. Rev. Lett. **97**, 045501 (2006).
[11] A. Ivanov and P. B. Littlewood, Phys. Rev. Lett. **87**, 136403 (2001).
[12] M. Lindberg and R. Binder, J. Phys. Condens. Matter **15**, 1119 (2003).
[13] R. Binder and M. Lindberg, J. Phys. Condens. Matter **18**, 729 (2006).
[14] M. Combescot, M. G. Moore, and C. Piermarocchi, Europhys. Lett. **93**, 47012 (2011).
[15] M. Combescot, M. G. Moore, and C. Piermarocchi, Phys. Rev. Lett. **106**, 206404 (2011).
[16] H. Yu, Y. Wang, Q. Tong, X. Xu, and W. Yao, Phys. Rev. Lett. **115**, 187002 (2015).
[17] F. Wu, T. Lovorn, and A. H. MacDonald, Phys. Rev. Lett. **118**, 147401 (2017).
[18] H. Yu, G. Liu, J. Tang, X. Xu, and W. Yao, Sci. Adv. **3**, e1701696 (2017).
[19] H. Guo, X. Zhang, and G. Lu, Sci. Adv. **6**, eabc5638 (2020).
[20] K. L. Seyler, P. Rivera, H. Yu, N. P. Wilson, E. L. Ray, D. G. Mandrus, J. Yan, W. Yao, and X. Xu, Nature (London) **567**, 66 (2019).
[21] C. Jin, E. C. Regan, A. Yan, M. I. B. Utama, D. Wang, S. Zhao, Y. Qin, S. Yang, Z. Zheng, S. Shi, K. Watanabe, T. Taniguchi, S. Tongay, A. Zettl, and F. Wang, Nature (London) **567**, 76 (2019).
[22] H. Baek, M. Brotons-Gisbert, Z. X. Koong, A. Campbell, M. Rambach, K. Watanabe, T. Taniguchi, and B. D. Gerardot, Sci. Adv. **6**, eaba8526 (2020).
[23] Y. Bai, L. Zhou, J. Wang, W. Wu, L. J. McGilly, D. Halbertal, C. F. B. Lo, F. Liu, J. Ardelean, P. Rivera, N. R. Finney, X. Yang, D. N. Basov, W. Yao, X. Xu, J. Hone, A. N. Pasupathy, and X.-Y. Zhu, Nat. Mat. **19**, 1068 (2020).
[24] C. Gardiner and P. Zoller, *Book I: Foundations of Quantum Optics* (Imperial College Press, London, 2014).
[25] C. Gardiner and P. Zoller, *Book II: The Physics of Quantum-Optical Devices* (Imperial College Press, London, 2015).
[26] R. D. King-Smith and D. Vanderbilt, Phys. Rev. B **47**, 1651(R) (1993).
[27] R. Resta, Rev. Mod. Phys. **66**, 899 (1994).
[28] See Supplemental Material at http://link.aps.org/supplemental/10.1103/PhysRevLett.129.047401 for the

information of the numerical convergence of GW + BSE calculations, the detailed derivation of Eq. (5), and the numerical convergence of Eq. (5).
[29] T. Fukui, Y. Hatsugai, and H. Suzuki, J. Phys. Soc. Jpn. **74**, 1674 (2005).
[30] H. Sahin, O. Leenaerts, S. K. Singh, and F. M. Peeters, WIREs Comp. Mol. Sci. **5**, 255 (2015).
[31] D. C. Elias, R. R. Nair, T. M. G. Mohiuddin, S. V. Morozov, P. Blake, M. P. Halsall, A. C. Ferrari, D. W. Boukhvalov, M. I. Katsnelson, A. K. Geim, and K. S. Novoselov, Science **323**, 610 (2009).
[32] M. M. S. Abdelnabi, C. Izzo, E. Blundo, M. G. Betti, M. Sbroscia, G. Di Bella, G. Cavoto, A. Polimeni, I. García-Cortés, I. Rucandio, A. Moroño, K. Hu, Y. Ito, and C. Mariani, Nanomater. Nanotechnol. **11**, 130 (2021).
[33] P. Giannozzi *et al.*, J. Phys. Condens. Matter **21**, 395502 (2009).
[34] S. Goedecker, M. Teter, and J. Hutter, Phys. Rev. B **54**, 1703 (1996).
[35] C. Hartwigsen, S. Goedecker, and J. Hutter, Phys. Rev. B **58**, 3641 (1998).
[36] J. Deslippe, G. Samsonidze, D. A. Strubbe, M. Jain, M. L. Cohen, and S. G. Louie, Comput. Phys. Commun. **183**, 1269 (2012).
[37] P. Cudazzo, C. Attacalite, I. V. Tokatly, and A. Rubio, Phys. Rev. Lett. **104**, 226804 (2010).
[38] S. Lebègue, M. Klintenberg, O. Eriksson, and M. I. Katsnelson, Phys. Rev. B **79**, 245117 (2009).
[39] F. Karlicky, R. Zboril, and M. Otyepka, J. Chem. Phys. **137**, 034709 (2012).
[40] O. Leenaerts, H. Peelaers, A. D. Hernandez-Nieves, B. Partoens, and F. M. Peeters, Phys. Rev. B **82**, 195436 (2010).
[41] A. Fetter and J. D. Walecka, *Quantum Theory of Many Particle Systems* (McGraw-Hill Book Company, San Francisco, 1971), pp. 538–539.
[42] A tiny gap breaking the degeneracy of E_u excitons is reported in [37] as well, we however point out that this is probably due to the symmetry violation by k point interpolation scheme in [36]. We confirmed the gap vanishes without such interpolation in $18 \times 18 \times 1$ k point calculation. We hence neglect the gap in this Letter.
[43] P. G. Eliseev, H. Li, A. Stintz, G. T. Liu, T. C. Newell, K. J. Malloy, and L. F. Lester, Appl. Phys. Lett. **77**, 262 (2000).
[44] T. H. Stievater, X. Li, D. G. Steel, D. Gammon, D. S. Katzer, D. Park, C. Piermarocchi, and L. J. Sham, Phys. Rev. Lett. **87**, 133603 (2001).
[45] K. Bergmann, H. Theuer, and B. W. Shore, Rev. Mod. Phys. **70**, 1003 (1998).
[46] S. Danisch and J. Krumbiegel, J. Open Source Softwaare **6**, 3349 (2021).
[47] P. Cudazzo, L. Sponza, C. Giorgetti, L. Reining, F. Sottile, and M. Gatti, Phys. Rev. Lett. **116**, 066803 (2016).
[48] Y. Yang, Y. Li, Z. Huang, and X. Huang, Carbon **107**, 154 (2016).
[49] D. Bousa, J. Luxa, D. Sedmidubsky, S. Huber, O. Jankovsky, M. Pumera, and Z. Sofer, RSC Adv. **6**, 6475 (2016).
[50] Y. Shi, H. Li, and L.-J. Li, Chem. Soc. Rev. **44**, 2744 (2015).
[51] C. Tan, X. Cao, X.-J. Wu, Q. He, J. Yang, X. Zhang, J. Chen, W. Zhao, S. Han, G.-H. Nam, M. Sindoro, and H. Zhang, Chem. Rev. **117**, 6225 (2017).
[52] W. Choi, N. Choudhary, G. H. Han, J. Park, D. Akinwande, and Y. H. Lee, Mat. Today **20**, 116 (2017).
[53] J. Son, S. Lee, S. J. Kim, B. C. Park, H.-K. Lee, S. Kim, J. H. Kim, B. H. Hong, and J. Hong, Nat. Commun. **7**, 13261 (2016).
[54] J. Sturala, J. Luxa, M. Pumera, and Z. Sofer, Chem. Eur. J. **24**, 5992 (2018).
[55] J. Zipfel, M. Kulig, R. Perea-Causín, S. Brem, J. D. Ziegler, R. Rosati, T. Taniguchi, K. Watanabe, M. M. Glazov, E. Malic, and A. Chernikov, Phys. Rev. B **101**, 115430 (2020).
[56] M. Kulig, J. Zipfel, P. Nagler, S. Blanter, C. Schüller, T. Korn, N. Paradiso, M. M. Glazov, and A. Chernikov, Phys. Rev. Lett. **120**, 207401 (2018).
[57] L. M. Smith, D. R. Wake, J. P. Wolfe, D. Levi, M. V. Klein, J. Klem, T. Henderson, and H. Morkoç, Phys. Rev. B **38**, 5788 (1988).
[58] H. Hillmer, S. Hansmann, A. Forchel, M. Morohashi, E. Lopez, H. P. Meier, and K. Ploog, Appl. Phys. Lett. **53**, 1937 (1988).
[59] S. Moritsubo, T. Murai, T. Shimada, Y. Murakami, S. Chiashi, S. Maruyama, and Y. K. Kato, Phys. Rev. Lett. **104**, 247402 (2010).
[60] A. D. Hernández-Nieves, B. Partoens, and F. M. Peeters, Phys. Rev. B **82**, 165412 (2010).
[61] H. Şahin, C. Ataca, and S. Ciraci, Phys. Rev. B **81**, 205417 (2010).
[62] P. Cudazzo, I. V. Tokatly, and A. Rubio, Phys. Rev. B **84**, 085406 (2011).
[63] F. Katsch, M. Selig, and A. Knorr, Phys. Rev. Lett. **124**, 257402 (2020).
[64] M. M. Ugeda, A. J. Bradley, S.-F. Shi, F. H. da Jornada, Y. Zhang, D. Y. Qiu, W. Ruan, S.-K. Mo, Z. Hussain, Z.-X. Shen, F. Wang, S. G. Louie, and M. F. Crommie, Nat. Mater. **13**, 1091 (2014).
[65] A. J. Bradley, M. M. Ugeda, F. H. da Jornada, D. Y. Qiu, W. Ruan, Y. Zhang, S. Wickenburg, A. Riss, J. Lu, S.-K. Mo, Z. Hussain, Z.-X. Shen, S. G. Louie, and M. F. Crommie, Nano Lett. **15**, 2594 (2015).
[66] H.-Y. Chen, D. Sangalli, and M. Bernardi, Phys. Rev. Lett. **125**, 107401 (2020).
[67] D. Y. Qiu, T. Cao, and S. G. Louie, Phys. Rev. Lett. **115**, 176801 (2015).
[68] M. Palummo, M. Bernardi, and J. C. Grossman, Nano Lett. **15**, 2794 (2015).
[69] L. Yuan, T. Wang, T. Zhu, M. Zhou, and L. Huang, J. Phys. Chem. Lett. **8**, 3371 (2017).